



# Application of New Co-simulation in System Simulation of Doubly-fed Induction Generator

Wen Jie Zheng, De Rui Dai, Gui Ji Tang\*

Department of Mechanical Engineering, North China Electric Power University, Baoding, China

## Email address:

[tanggjlk@ncepu.edu.cn](mailto:tanggjlk@ncepu.edu.cn) (Gui Ji Tang)

\*Corresponding author

## To cite this article:

Wen Jie Zheng, De Rui Dai, Gui Ji Tang. Application of New Co-simulation in System Simulation of Doubly-fed Induction Generator. *International Journal of Electrical Components and Energy Conversion*. Special Issue: *Electro-Mechanical Coupling Problems in Electric Machines*. Vol. 7, No. 2, 2021, pp. 54-60. doi: 10.11648/j.ijecec.20210702.14

**Received:** November 24, 2021; **Accepted:** December 16, 2021; **Published:** December 29, 2021

---

**Abstract:** This paper proposes a doubly-fed induction generator (DFIG) model built on three simulation platforms: Maxwell, Simplorer and Simulink. It can solve the overall modeling problem of the DFIG system effectively. In this paper, the generator physical simulation model (rotating shaft, rotor, stator and winding) are first established in Maxwell. Then, the internal (stator/rotor winding) and external circuit of DFIG are connected in Simplorer. The external circuit includes converter (generator side and grid side), filter, transformer and grid. Moreover, both the generator-side converter and the grid-side converter are controlled by Simulink. Finally, the simulation calculation study on the 5.5kW DFIG are carried out to validate the theoretical analysis. It is shown that SAGE causes distortion of the air gap magnetic field, the magnetic flux density (MFD) is inversely related to air gap changes. In addition, with the increase of SAGE, the curve of electromagnetic torque (EMT) moves down and rotor unbalanced magnetic pull (UMP) fluctuations become more obvious. The model can simulate the DFIG system accurately and effectively. And the simulation results are consistent with the theoretical derivation, which proves the validity of the model. This provides an effective method for the whole simulation and fault analysis of DFIG system.

**Keywords:** Doubly-fed Induction Generator (DFIG), Co-simulation, Fault Diagnosis, Static Air-gap Eccentricity (SAGE)

---

## 1. Introduction

Wind power technology has gradually become a key research topic worldwide gradually, because wind energy has the advantages of being clean, green and pollution-free [1, 2]. In recent years, the wind power industry has developed rapidly, and wind power has become one of the main power sources of power system [3]. But at the same time, there are also some technical problems that need to be overcome. For example, the winding vibration and wear problems caused by various complex factors such as wind speed and climate change [4], aerodynamic asymmetry [5], and transmission chain component failure [6] need to be solved urgently. In addition, the insulation degradation and damage of wind turbine windings under grid-side imbalance [7] and fault impact [8] also need to be studied.

In fact, the entire process of a doubly-fed induction generator from the impeller capturing wind energy to obtain mechanical torque until the generator outputs electrical

energy is an energy transmission chain. The two ends of this transmission chain, namely the mechanical end and electrical end, may input unstable shocks to the generator (such as aerodynamic asymmetry and grid short circuit) [9]. If the failure is allowed to develop, the generator may cause irreversible damage under the cumulative effect. There are mainly six typical unstable shocks such as aerodynamic asymmetry, bearing failure, gear failure, low voltage ride-through [10], sub synchronous resonance [11] and grid short circuit.

In order to reduce the cost of wind power generation and improve the efficiency of wind energy utilization, the single-unit capacity of wind power generation equipment is increasing. Therefore, more research is needed on the design and manufacture of wind turbines, control system design and operation and other aspects. Simulation technology has gradually been widely used in the field of research and testing of wind turbines because of its strong adaptability and low cost.

Most of the traditional generator simulation is to use one of Matlab-Simulink, Maxwell and other software to realize the modeling and simulation of the generator system [12, 13]. Although some results have been achieved, it cannot reflect the actual working conditions of the generator completely and accurately. It is undeniable that Matlab has considerable performance in terms of control principles, but there are certain defects in generator transmission [14]. Specifically, applying the state-space equation method to establish a generator model in Simulink and using some of the power electronic devices and generator models provided by the existing Power Blocks module in Simulink can be used for generator control system simulation. However, Simulink simulation cannot reflect the real-time state of the motor. Because it can only provide static power electronic devices and linear motor models, it can be used for evaluation of control algorithms, but it cannot constitute a real controller design and overall policy [15-17]. Maxwell is typical electromagnetic finite element analysis software, which can realize the analytical calculation of motor performance and automatically generate Maxwell 2D/3D finite element model. Maxwell can perform finite element analysis on the transient and steady state of the motor, and realize the optimal design of the motor. However, it has limitations in the control algorithm and cannot complete the design and implementation of the algorithm for complex motor control strategies (such as fuzzy controllers, etc.) [18].

In response to the above problems, this paper proposes a simulation method that can reflect the actual working conditions of the motor quickly and control the motor in real time, that is, use Maxwell, Simplorer and Simulink three software for co-simulation. In order to verify the effectiveness of the simulation platform, the joint simulation

models of doubly-fed induction generators under normal and eccentric conditions based on these three soft wares was built. The simulation results are closer to the actual operating conditions of the generator. The platform construction process is as follows: First, Maxwell is used to design a simulation model of a doubly-fed induction generator to reflect the actual working conditions of the generator. Then set up the circuit of generator system in Simplorer, and transfer data (such as the generator speed and current) in Maxwell to Simulink. Then a control circuit was built in Simulink to control the converter and protection device in Simplorer. Finally, run the joint simulation in Simplorer, and the results of the simulation can be viewed in Maxwell or Simplorer.

## 2. Establishment of DFIG Co-simulation Model

The control structure of the wind power plant is shown in Figure 1. The blades capture wind energy and use the gearbox to drive the rotor of the generator to rotate to generate electricity. The generator studied in this paper is DFIG, whose rotor windings only play an excitation role at sub-synchronous speed and synchronous speed. But when the rotor speed of DFIG is in a super-synchronous state, the rotor windings also play a role in power transmission to the grid. This requires a control system to accurately control the generator rotor winding circuit at various wind speeds. The co-simulation model in this article solves the simulation problem of generator model and grid-connected circuit and its control.

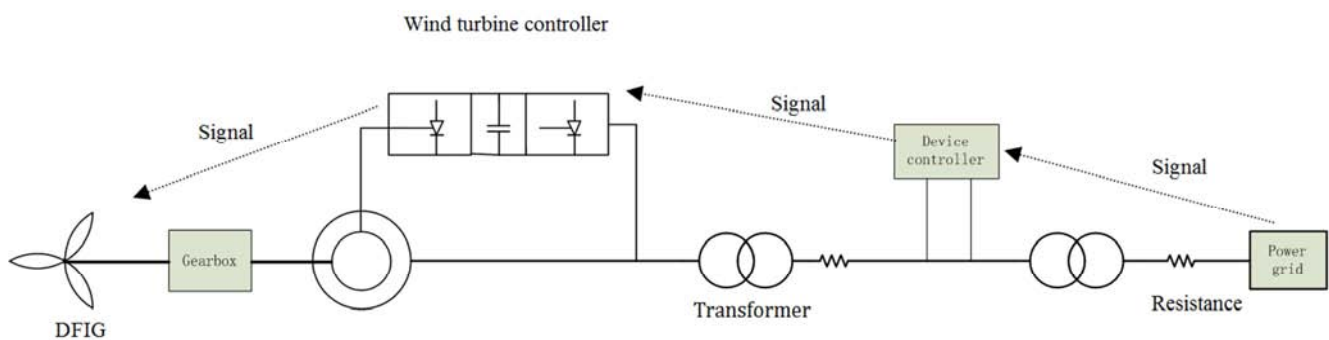


Figure 1. DFIG system.

The simulation in this article is divided into three modules, namely Maxwell, Simplorer and Simulink. Maxwell was used to build a specific model of DFIG in actual operation. Simplorer is used to build specific circuits in the process of DFIG grid connection. Simulink is used to build a control circuit that controls the generator side/grid-side converter in Simplorer.

### 2.1. The Maxwell Model of DFIG Under Normal and SAGE Conditions

This article takes DFIG under normal and SAGE

conditions as an example to establish a simulation model, and the normal and fault conditions are shown in Figure 2. According to literature [19], static air-gap eccentricity (SAGE) mainly affects the permeance per unit area (PPUA), and no influence on the magnetic motive force (MMF). Magnetic flux density (MFD) is composed of MMF and PPUA. The MFD can be expressed by Eq. 1 under normal and SAGE (ignoring the change of PPUA caused by the interaction of the stator and rotor slots).

$$\begin{cases} b(\alpha_m, t) = f(\alpha_m, t) \Lambda(\alpha_m, t) = \left[ f_p(\alpha_m, t) + \sum_v f_v(\alpha_m, t) + \sum_\mu f_\mu(\alpha_m, t) \right] \times \left[ \Lambda_0 + \sum_{k_1} \lambda_{k_1} + \sum_{k_2} \lambda_{k_2} + \sum_{k_1, k_2} \lambda_{k_1} \lambda_{k_2} \right] \cdots \text{normal} \\ b_e(\alpha_m, t) = f(\alpha_m, t) \Lambda_e(\alpha_m, t) = \left[ f_p(\alpha_m, t) + \sum_v f_v(\alpha_m, t) + \sum_\mu f_\mu(\alpha_m, t) \right] \times \left[ (\Lambda_0 + \sum_{k_1} \lambda_{k_1} + \sum_{k_2} \lambda_{k_2} + \sum_{k_1, k_2} \lambda_{k_1} \lambda_{k_2}) (1 + \delta_s \cos \alpha_m + \delta_s^2 \cos^2 \alpha_m) \right] \cdots \text{SAGE} \end{cases} \quad (1)$$

where  $f_p(\alpha_m, t)$ ,  $f_v(\alpha_m, t)$  and  $f_\mu(\alpha_m, t)$  are respectively the main wave synthetic magnetic potential, the stator winding harmonic magnetic potential and the rotor winding harmonic magnetic potential.  $p$  is the main wave synthetic magnetic the number of pole pairs of the potential.  $v$  and  $\mu$  are the pole pairs of the stator and rotor winding tooth harmonic magnetic potential respectively.  $\alpha_m$  is the circumferential angle of the air gap.  $t$  is the time.  $\Lambda_0$  is the constant part of the air gap permeance.  $\lambda_{k1}$  is the harmonic permeance caused when the stator is slotted and the rotor surface is smooth.  $\lambda_{k2}$  is the harmonic permeance caused when the rotor is slotted and the stator surface is smooth.  $\lambda_{k1}\lambda_{k2}$  is the harmonic permeance caused by the simultaneous slotting interaction of the stator and rotor.  $\delta_s$  is the value of rotor static eccentricity,  $\delta_s = |OO'|/g_0$ , as shown in Figure 2.

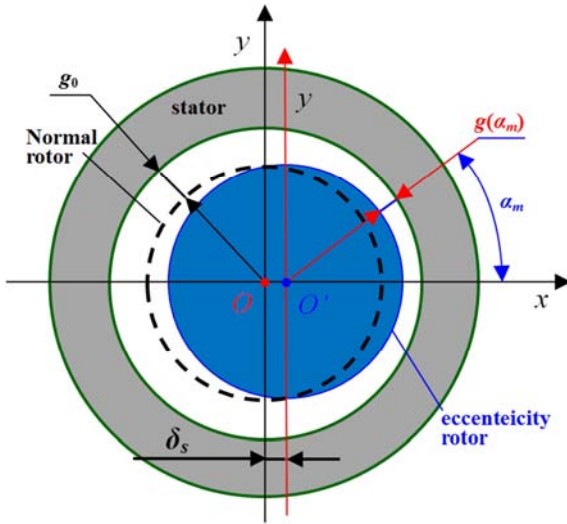


Figure 2. Air-gap of generator in normal and SAGE.

Ignore the high-order and small amplitude harmonics, the Electromagnetic torque (EMT) can be written as [20]

$$T_{em} = \frac{ml^2 R_s^2 \pi n_r \cos \varphi}{30Z} b^2(\alpha_m, t) \quad (2)$$

where  $m$  is the number of phases,  $\varphi$  is the power factor angle.  $l$  is the effective length of the stator winding within the magnetic field.  $R_s$  is the inner diameter of the stator core.  $n_r$  is the speed of the generator rotor.  $Z$  is the total reactance of the stator winding.

Generally, the magnetic pull per unit area (MPPUA) generated by MFD contains radial and circumferential components. Circumferential MPPUA has little effect, so radial MPPUA is taken into account. According to Maxwell tensor method, the value of radial MPPUA in the air gap can be expressed as

$$q(\alpha_m, t) = \frac{b^2(\alpha_m, t)}{2\mu_0} \quad (3)$$

The radial unbalanced magnetic pull (UMP) of the rotor can be obtained through [21]

$$\begin{cases} F_x = LR \int_0^{2\pi} q(\alpha_m, t) \cos \alpha_m d\alpha_m \\ F_y = LR \int_0^{2\pi} q(\alpha_m, t) \sin \alpha_m d\alpha_m \end{cases} \quad (4)$$

From Eq. 1, the air gap MFD under SAGE is  $(1 + \delta_s \cos \alpha_m + \delta_s^2 \cos^2 \alpha_m)$  more than normal. Therefore, the MFD after eccentricity is related to  $\alpha_m$ . Specifically, MFD decreases as the air gap increases, and increases as the air gap decreases. And the EMT will increase (see Eq. 2). The EMT of the generator is negative, so the occurrence of SAGE reduces the torque. According to Eq. 4, the rotor unbalanced magnetic pull (UMP) is zero under normal conditions, and the rotor has no vibration. After eccentricity, the magnetic field distribution is not uniform, and UMP increases.

Table 1. Basic parameters of 5.5kW doubly fed induction generator.

Parameters	Value
Rated Capacity	5.5kW
Rated voltage	380 V
Frequency	50 Hz
Power efficiency	0.94
Rated rotating speed	1500 rpm
Outer diameter of stator core	210 mm
Inner diameter of stator core	136 mm
Out diameter of rotor core	134 mm
Inner diameter of rotor core	48 mm
Length	155 mm
Stator/Rotor slots	36/24
Stator/Rotor Pole pairs	2/2

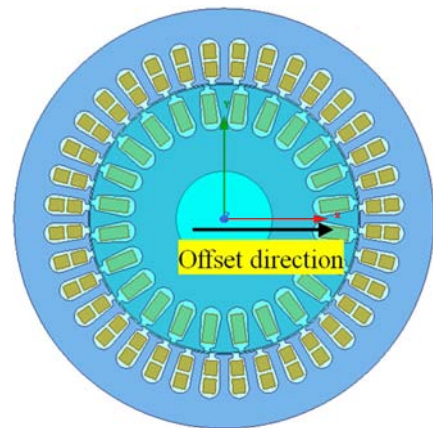


Figure 3. Maxwell model.

The simulation is based on a 5.5kW DFIG. The physical and structural parameters of the generator are shown in Table 1. Input the generator parameters in the RMxp module in Maxwell, and directly generate the required two-dimensional finite element model of the generator, as shown in Figure 3.

The stator and rotor winding excitation is external excitation, and check the box in front of "Enable transient-transient link with Simplorer". The appropriate step size is selected during co-simulation (the step size in Maxwell is smaller than it in Simplorer). In this paper, the calculation stop time of the Maxwell model is 2s, and the step size is 2ms. The SAGE faults of DFIG (generally caused by aerodynamic asymmetry, bearing failure, etc.) can be implemented by the eccentricity command in the Maxwell. Figure 4 shows the direction of the rotor eccentricity.

In this paper, the degree of SAGE is set to 0.1mm, 0.2mm, 0.3mm along the X direction, so three simulation models with different degrees of eccentricity are obtained. Eccentricity failure will only change the air gap distribution between the stator and rotor. It has no effect on the external

winding connection mode, so the circuit connection in Simplorer remains unchanged.

After building the generator model in Maxwell, the model was imported into Simplorer and connected to the external circuit.

## 2.2. The Establishment of Control Circuit Model in Simplorer

In the establishment of the Simplorer model, the stator winding of the generator can be directly connected to the grid. However, the rotor winding must be converted and filtered before it can be connected to the grid (the rotor winding not only has the excitation function, but also can provide electric energy to the grid when the wind speed is high). The specific circuit connection is shown in Figure 4. The name of each interface in the model is determined according to the example of DFIG in Matlab.

As shown in Figure 4, the basic control system of DFIG includes filters (generator side and grid side), converter (machine side and grid side) and transformer.

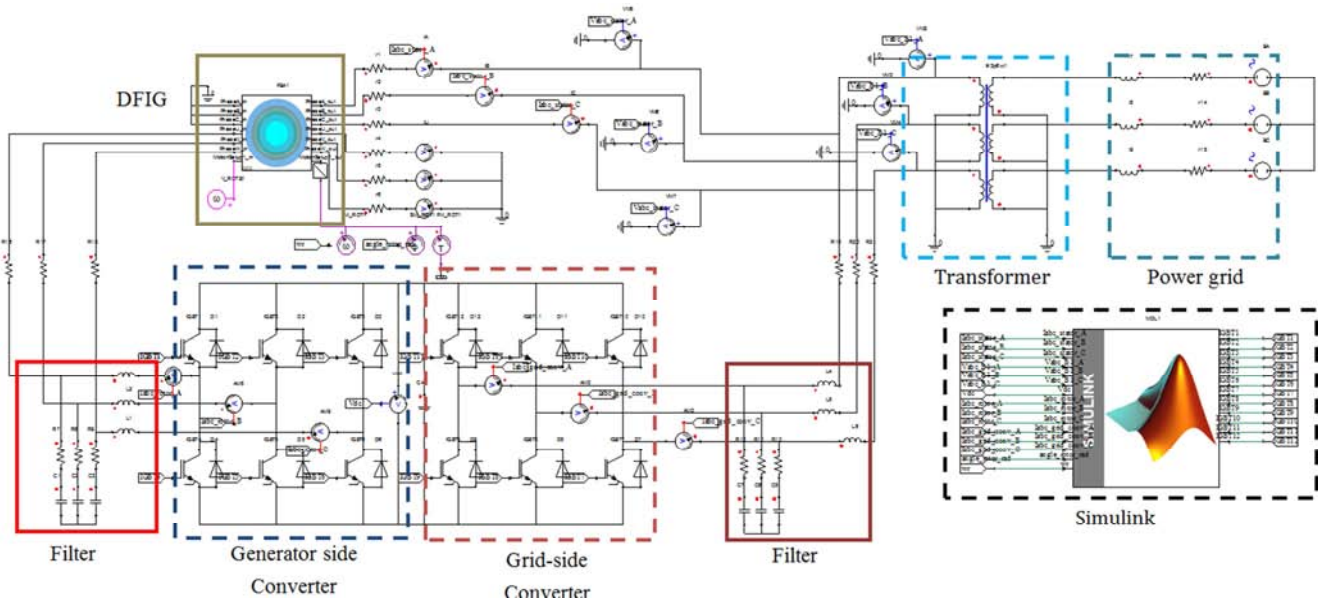


Figure 4. Simplorer model.

The converter is the core control component of the electrical part, divided into generator side converter and grid-side converter. The generator-side converter can realize variable-speed but constant-frequency operation of the wind power system by adjusting the frequency of the excitation current. The main purpose of the grid-side converter is to provide a stable DC-side voltage for the generator side converter, thereby realizing the two-way flow of power. These two parts are combined by Insulated Gate Bipolar Transistor (IGBT). And the specific control of IGBT is completed by Simulink.

## 2.3. Establishment of Simulink Control Circuit

The connection between Simulink and Simplorer is

completed by the S-Function module in Simulink. Various data in Simplorer (such as rotor speed, rotation angle, current on the rotor side and grid side, etc.) are transmitted to Simulink, and then the control data of 12 IGBT ports is transmitted back after being processed by the control circuit.

The simulation time and step size of Simulink in this article are consistent with Simplorer. The control logic block diagram of the converter on the generator side and the grid side, as shown in Figure 5, and the simulation module built in Simulink, as shown in Figure 6.

According to Figure 6, the currents of the rotor-side winding, the stator-side winding and the grid-side circuit, the voltage between the two converters, and the rotor speed and rotation angle of the DFIG are all received as input signals by



Simulink. After the signal is processed by the control circuit in the module, the information for controlling each IGBT interface in Simplorer is obtained.

At this point, the co-simulation model has been established.

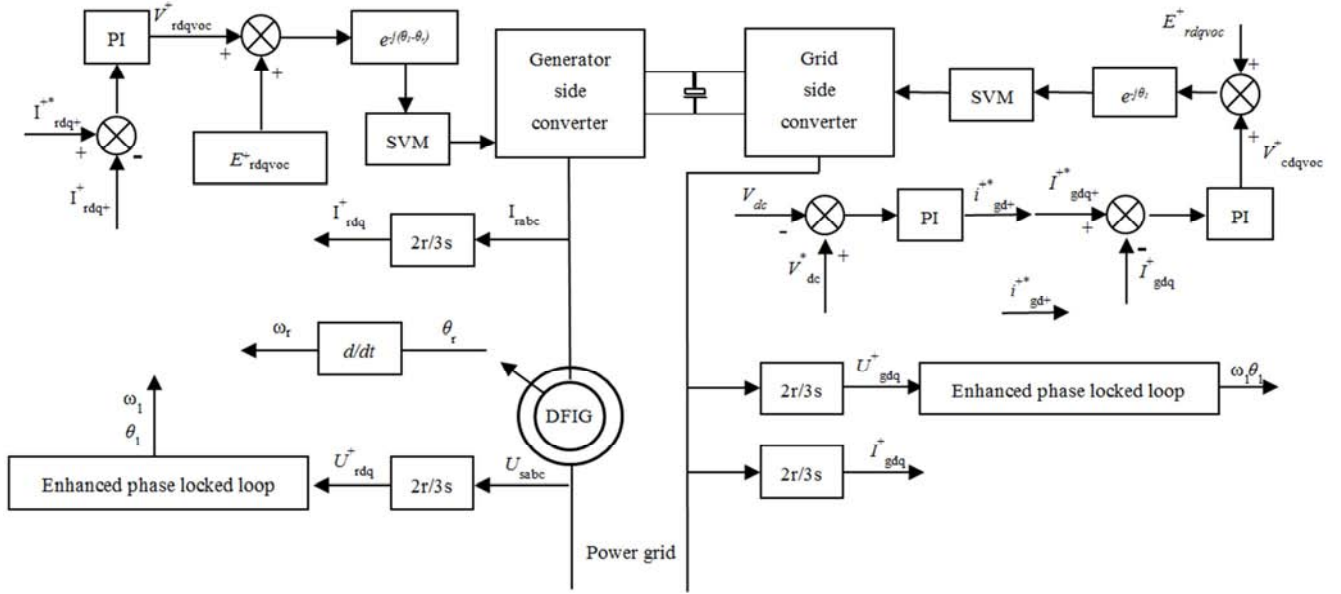


Figure 5. Converter control block diagram.

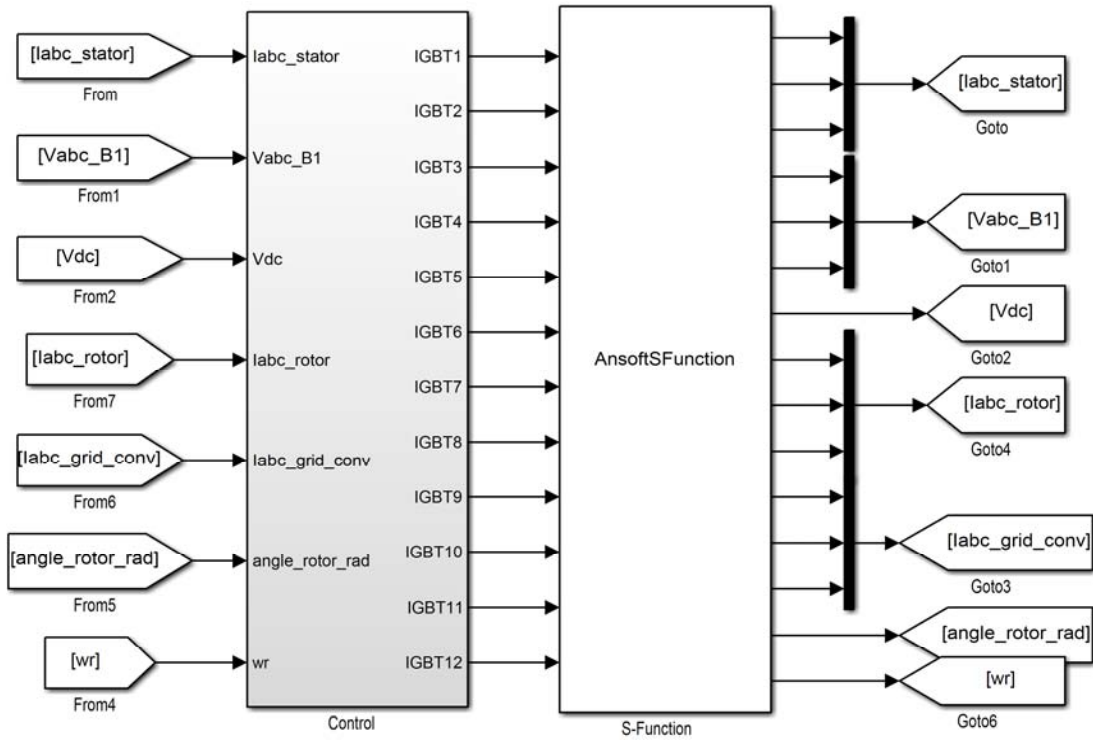


Figure 6. Simulink model.

### 3. Results and Discussion

The simulation results can be viewed in Simplorer or Maxwell. Figure 7 is the MFD of DFIG, and Figure 8 is the EMT diagram of the generator. Figure 9 shows the UMP of the rotor. The above results are all obtained under normal and

different eccentricity conditions of DFIGURE.

According to Figure 7, the MFD is distributed symmetrically and has two cycles (the DFIG simulated in this paper is a generator with two pairs of poles) when the DFIG is running normally. But the MFD will be distorted after eccentricity. Specifically, the MFD on the side where the air gap decreases is increased, and the MFD on the side

where the air gap increases decreases.

In addition, the simulated EMT is fluctuate value in a no stable (as Figure 8). But eventually it will stabilize, and it is negative value. This is because the asynchronous electric machine in this article is in the generator state and the torque is the resistance torque. And the torque decreases with the increase of eccentricity.

Moreover, the rotor is basically free of vibration in normal operation. The occurrence of eccentricity will increase the UMP of the rotor, which will cause the rotor to vibrate. And the vibration increases with the increase of eccentricity, as shown in Figure 9. The above simulation results are consistent with the theoretical analysis.

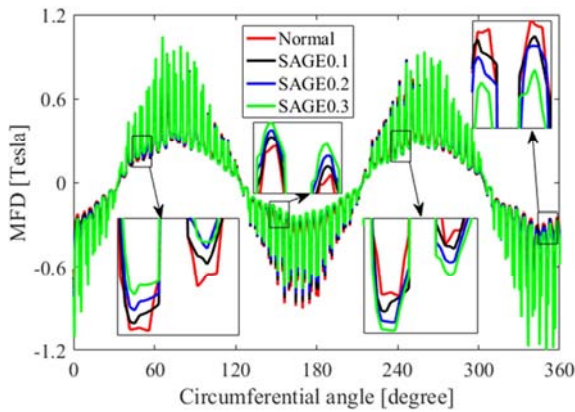


Figure 7. Spatial distribution of MFD before and after SAGE.

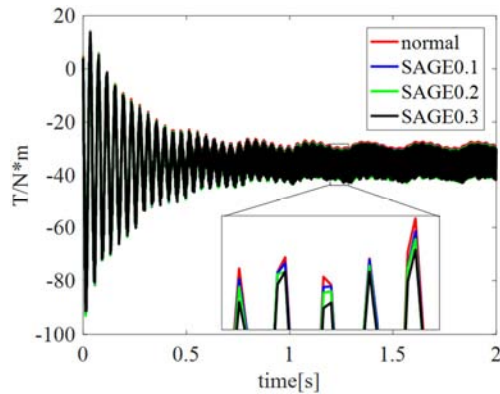


Figure 8. Time domain waves of torque before and after SAGE.

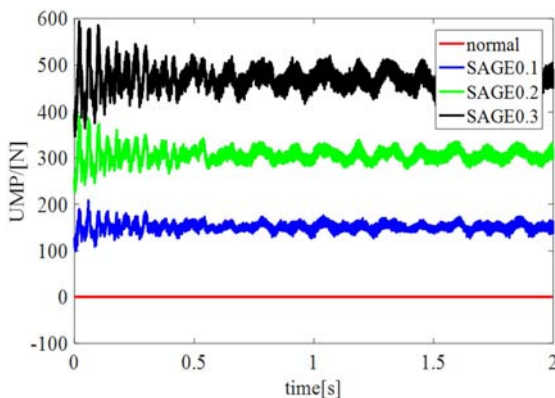


Figure 9. UMP of rotor before and after SAGE.

## 4. Conclusion

This paper proposes a simulation model integrating Maxwell, Simplorer and Simulink, which can effectively solve the problems of DFIG physical simulation, converter control and generator grid connection. It can not only see the changes of basic parameters (current, EMT, etc.) during DFIG operation, but also more intuitively simulate the influence of generator-side SAGE fault on the MFD and rotor vibration of DFIGURE.

- (1) The co-simulation model can better simulate the situation of the real generator system, including generator model, converter and its control, grid operation, etc.
- (2) The co-simulation model can more effectively simulate the faults on DFIGURE This article gives an example of simulating radial eccentricity. The results are consistent with the theoretical analysis, indicating the effectiveness of the model.

## Acknowledgements

This work supported in part by National Natural Science Foundation of China (51777074, 52177042), in part by Natural Science Foundation of Hebei Province, China (E2020502031), in part by the Chinese Fundamental Research Funds for the Central Universities (2020MS114, 2018YQ03), and in part by the 3<sup>rd</sup> Top Youth Talent Support Program of Hebei Province ([2018]-27).

## References

- [1] M. A. Ortega-Vazquez and D. S. Kirschen (2009). "Estimating the Spinning Reserve Requirements in Systems With Significant Wind Power Generation Penetration". *IEEE Transactions on Power Systems*; 24 (1): 114-124.
- [2] M. Yin, Y. Xu, C. Shen, J. Liu, Z. Y. Dong and Y. Zou (2017). "Turbine Stability-Constrained Available Wind Power of Variable Speed Wind Turbines for Active Power Control". *IEEE Transactions on Power Systems*; 32 (3): 2487-2488.
- [3] Yuan J, Na C, Xu Y, et al (2015). "Wind turbine manufacturing in China: A review". *Renewable and Sustainable Energy Reviews*; 51: 1235-1244.
- [4] X. Xing, H. Meng, L. Xie, L. Yue and Z. Lin (2019). "Switching Performance Improvement Based on Model-Predictive Control for Wind Turbine Covering the Whole Wind Speed Range". *IEEE Transactions on Sustainable Energy*; 10 (1): 290-300.
- [5] Niebsch J, Ramlau R, Nguyen T T (2010). "Mass and Aerodynamic Imbalance Estimates of Wind Turbines". *Energies*; 3 (4): 696-710.
- [6] X. Rui, L. Li and X. Li (2008). "Fundamentals of a power splitting driving chain for large wind turbines". *2008 7<sup>th</sup> World Congress on Intelligent Control and Automation*; 9347-9350.
- [7] A. E. Leon, J. M. Mauricio and J. A. Solsona (2012). "Fault Ride-Through Enhancement of DFIG-Based Wind Generation Considering Unbalanced and Distorted Conditions". *IEEE Transactions on Energy Conversion*; 27 (3): 775-783.

- [8] A. H. Soloot, H. K. Høidalen and B. Gustavsen (2015). "Influence of the winding design of wind turbine transformers for resonant overvoltage vulnerability". *IEEE Transactions on Dielectrics and Electrical Insulation*; 22 (2): 1250-1257.
- [9] Sheng XL, Wan ST, Cheng LF, Li YG (2017). "Blade aerodynamic asymmetry fault analysis and diagnosis of wind turbines with doubly fed induction generator". *Journal of Mechanical Science And Technology*; 31 (10): 5011-5020.
- [10] T. Qiu, X. Wang, Q. Yin and D. Wang (2021). "Research on Precise Voltage Regulation Control Strategy of High and Low Voltage Ride Through Test Device of Inverter". *2021 6<sup>th</sup> Asia Conference on Power and Electrical Engineering (ACPEE)*; 944-948.
- [11] S. Rezaei (2017). "Behavior of protective relays during Sub Synchronous Resonance". *2017 IEEE International Conference on Environment and Electrical Engineering and 2017 IEEE Industrial and Commercial Power Systems Europe (EEEIC/ I&CPS Europe)*; 1-5.
- [12] J. Shi, Y. Tang, Y. Xia, L. Ren and J. Li (2011). "SMES Based Excitation System for Doubly-Fed Induction Generator in Wind Power Application". *IEEE Transactions on Applied Superconductivity*; 21 (3): 1105-1108.
- [13] Y. -L. He *et al.* (2019). "Effect of 3D Unidirectional and Hybrid SAGE on Electromagnetic Torque Fluctuation Characteristics in Synchronous Generators". *IEEE Access*; 7: 100813-100823.
- [14] L. Yuegang, X. Peiyu, L. Nailu and F. Xiaoxu (2009). "Research of VSCF wind power generation training system based on matlab/labVIEW". *2009 IEEE International Conference on Automation and Logistics*; 1592-1597.
- [15] Z. Sun, H. Wang and Y. Li (2012). "Modelling and simulation of doubly-fed induction wind power system based on Matlab/Simulink". *International Conference on Sustainable Power Generation and Supply (SUPERGEN 2012)*; 1-5.
- [16] J. S. Solanke, A. V. Naik and B. T. Deshmukh (2016). "Coordination control of DFIG under distorted grid voltage conditions using Matlab-simulink". *2016 International Conference on Computing Communication Control and automation (ICCCBEA)*; 1-6.
- [17] T. Jiang and Y. Zhang (2021), "Robust Predictive Rotor Current Control of Doubly Fed Induction Generator under Unbalanced and Distorted Grid," in *IEEE Transactions on Energy Conversion*, doi: 10.1109/TEC.2021.3104410.
- [18] Y. He, Y. Zhang, M. Xu, X. Wang and J. Xiong (2019), "A New Hybrid Model for Electromechanical Characteristic Analysis Under SISC in Synchronous Generators," in *IEEE Transactions on Industrial Electronics*, 67 (3): 2348-2359.
- [19] Di Chong, Bao Xiaohua, Wang Hanfeng, Fang Yong, Zhu Qinglong (2014). "Research on radial electromagnetic excitation force of induction motor with mixed eccentricity," *Transactions of China Electrotechnical society*, 29 (S1): 138-144.
- [20] TANG Yunqiu (2011). "Electrical machinery. 4<sup>th</sup> Edition," Machinery industry press.
- [21] He, Y. L., Ke, M. Q., Wang, F. L., et al (2015). "Effect of static eccentricity and stator inter-turn short circuit composite fault on rotor vibration characteristics of generator," *Trans. Can. Soc. for Mech. Eng.* 39 (4): 767-781.